Eur. Phys. J. C (2011) 71:1756
DOI 10.1140/epjc/s10052-011-1756-5

THE EUROPEAN PHYSICAL JOURNAL C

Regular Article - Theoretical Physics

Complex Langevin: etiology and diagnostics of its main problem

Gert Aarts[1,a], **Frank A. James**[1,b], **Erhard Seiler**[2,c], **Ion-Olimpiu Stamatescu**[3,d]

[1]Department of Physics, Swansea University, Swansea, UK
[2]Max-Planck-Institut für Physik (Werner-Heisenberg-Institut), München, Germany
[3]Institut für Theoretische Physik, Universität Heidelberg and FEST, Heidelberg, Germany

Received: 1 August 2011 / Revised: 5 September 2011

Abstract The complex Langevin method is a leading candidate for solving the so-called sign problem occurring in various physical situations. Its most vexing problem is that sometimes it produces 'convergence to the wrong limit'. In this paper we carefully revisit the formal justification of the method, identifying points at which it may fail and derive a necessary and sufficient criterion for correctness. This criterion is, however, not practical, since its application requires checking an infinite tower of identities. We propose instead a practical test involving only a check of the first few of those identities; this raises the question of the 'sensitivity' of the test. This sensitivity as well as the general insights into the possible reasons of failure (the etiology) are then tested in two toy models where the correct answer is known. At least in those models the test works perfectly.

1 Introduction

The sign problems arising in simulations of various systems, in particular in QCD with finite chemical potential [1], are in principle solved by using the complex Langevin equation (CLE). This method, after being proposed in the early 1980s by Klauder [2–4] and Parisi [5], enjoyed a certain limited popularity (see for instance [6, 7]) and has in more recent years been revived with some success [8–16]. Unfortunately already in the beginning problems were encountered. The first problem, instability of the simulations (runaways) can be dealt with by introducing an adaptive step size, as shown in [14]. More vexing is the second problem: convergence to a wrong limit [15, 17–20]. It is this problem which we wish to address in this paper.

A formal argument for correctness of the CLE was presented in a previous paper [21]. Here we analyze in more detail the possible failure of this argument and isolate a crucial identity that is necessary and sufficient for the correctness of the argument. The argument rests on the comparison of two time evolutions: the first one of a complex measure not allowing a probabilistic interpretation—the origin of the sign problem—the other one of a positive measure on a complexified space, allowing a probabilistic interpretation and hence suitable for simulation. The main point is that these two time evolutions should lead to identical evolutions for the expectation values of holomorphic observables. This implies of course also that the long-time limits (assuming their existence) agree and yield the desired equilibrium expectation values.

In [21] we already raised some questions concerning those formal arguments. Some of them are of a slightly academic nature, namely the mathematically sticky problem of the existence of those evolutions and their convergence properties. Taking a pragmatic attitude, these problems are answered by performing simulations; in a large set of examples the answer is positive. The remaining problem is much more insidious: it may (and sometimes it does) happen that the results of a simulation are well converged and look perfectly fine, but turn out to be wrong when compared with known results. This is the disease of 'convergence to the wrong limit'. Since the goal is to study models like finite density QCD in which the correct answer is not known, it is important to have diagnostic tools allowing an educated decision on whether to trust the results of a simulation or not. One of the goals of this paper is to arrive at practical criteria, which, when violated, indicate an incorrect answer.

To find diagnostic tools for a disease it helps to have a deeper understanding of its causes (the etiology). We identify in this paper two possible causes of the failure of the formal arguments: insufficient falloff of the probability distribution in the imaginary directions and too strong growth

[a] e-mail: g.aarts@swan.ac.uk
[b] e-mail: pyfj@swan.ac.uk
[c] e-mail: ehs@mppmu.mpg.de
[d] e-mail: I.O.Stamatescu@thphys.uni-heidelberg.de

Published online: 01 October 2011

of the (time-evolved) observables in the imaginary directions. These two phenomena can invalidate the integrations by parts which are necessary to show agreement of the two time evolutions mentioned above.

The plan of the paper is as follows: in Sect. 2 we revisit the formal argument and deduce the critical identity mentioned above; more precisely it is a set of identities, one for each observable. Section 3 considers the long-time limits of the two time evolutions. The identities of Sect. 2 lead in the long-time limit to a set of simpler ones which turn out to be closely related to the Schwinger–Dyson equations (SDE). We show that under some mild technical conditions the complete set of these identities, together with a certain bound, is not only necessary but also sufficient to establish correctness of the limit.[1]

In Sect. 4 we then study these issues in detail in two toy models. The first one is a one-link version of lattice U(1) gauge theory, already studied in [11, 21]; the second one, which was first studied by Guralnik and Pehlevan [22], is a polynomial model with purely imaginary action, which is a toy version of the real time Feynman path integral. To test both the etiology and the diagnostics, we make use of some parameters that can be tuned to produce correct results. The first one is the strength of the noise in the imaginary direction, which according to the formal argument can be chosen freely. The second one is taking advantage of the fact that the positive measure on the complexified field space is not uniquely determined by the complex measure on the real field space; concretely we introduce a field cutoff in imaginary direction and check whether it can be tuned to produce correct results.

Section 4.1 contains a detailed study of the identities necessary for the agreement of the two time evolutions for the U(1) one-link model, dependent on both parameters mentioned above. It turns out that in general the crucial identities are violated and the results are incorrect, except for either zero imaginary noise, or for nonzero imaginary noise and a special value of the cutoff. That we generally get wrong results with a cutoff in place is no surprise, since there is no formal argument for correctness. More surprising is the fact that even without cutoff we get wrong results as soon as there is an appreciable imaginary noise present. In the Appendix the reason for the failure is explained by looking at the growth of the (noise averaged) observables in imaginary direction, evolved for a finite amount of time. It turns out that these quantities show a dramatic growth in imaginary direction, which cannot be compensated by the decay of the probability measure; thus the formal argument becomes invalid.

[1]Logically it is conceivable, though highly improbable, that the two time evolutions disagree but lead to the same long-time limit; this would mean that the identities of Sect. 2 fail but those of Sect. 3 are valid.

In Sect. 4.2 we investigate the falloff of the equilibrium distribution in imaginary direction for both toy models; again it is found that in the presence of complex noise the falloff is insufficient for the derivation of the SDE identities. This corroborates in detail the indications presented in [21]. For purely real noise, on the contrary, the distributions show much stronger falloff, which is sufficient for the derivation of the SDE identities.

In Sect. 4.3 we use a truncated form of our SDE criterion as a test of correctness of the equilibrium measures in both of our toy models; it turns out that the test is surprisingly strong. To put it in terms of medical statistics: the test has perfect *specificity* (100%), i.e. when the simulation is correct, it is always fulfilled; this is a general mathematical fact. But the pleasant surprise is its very strong *sensitivity*, meaning that in the cases studied, when it is fulfilled, the results, as far as checked, are correct.

Finally in Sect. 5 we draw some conclusions and present an outlook on work in progress. A more detailed mathematical analysis concerning the U(1) one-link model is given in the Appendix.

2 The formal arguments revisited

We briefly go through the arguments presented in [21], concentrating on models in which the fields take values in flat manifolds $\mathcal{M}_r = \mathbb{R}^n$ or $\mathcal{M}_r = T^n$, where T^n is the n dimensional torus $(S^1)^n$ with coordinates $(x_1, \ldots, x_n)$.

The complex measure $\exp(-S)\,dx$, with S a holomorphic function on a real manifold $\mathcal{M}$, is replaced by a positive measure $P\,dx\,dy$ on the complexification $\mathcal{M}_c$ of $\mathcal{M}$, which is the equilibrium measure of the complex Langevin process on $\mathcal{M}_c$; the hope is that expectation values of *entire holomorphic observables* $\mathcal{O}$ agree with those obtained using the complex measure $\exp(-S)\,dx$.

The complex Langevin equation (CLE) on $\mathcal{M}_c$ is

$$\begin{aligned} dx &= K_x\,dt + \sqrt{N_R}\,dw_R, \\ dy &= K_y\,dt + \sqrt{N_I}\,dw_I, \end{aligned} \tag{1}$$

where dw_R and dw_I are independent Wiener processes, $N_I \geq 0$ and $N_R = N_I + 1$. In the case $N_I > 0$ we speak of complex noise. The drift is given by

$$\begin{aligned} K_x &= -\mathrm{Re}\nabla_x S(x+iy), \\ K_y &= -\mathrm{Im}\nabla_x S(x+iy). \end{aligned} \tag{2}$$

By Itô calculus, if f is a twice differentiable function on $\mathcal{M}_c$ and

$$z(t) = x(t) + iy(t) \tag{3}$$

is a solution of the complex Langevin equation (1), we have

$$\frac{d}{dt}\big\langle f\big(x(t),y(t)\big)\big\rangle = \big\langle Lf\big(x(t),y(t)\big)\big\rangle, \tag{4}$$

where L is the Langevin operator

$$L = [N_R\nabla_x + K_x]\nabla_x + [N_I\nabla_y + K_y]\nabla_y, \tag{5}$$

and $\langle f\rangle$ denotes the noise average of f corresponding to the stochastic process described by (1). In the standard way (1) leads to its dual Fokker–Planck equation (FPE) for the evolution of the probability density $P(x,y;t)$,

$$\frac{\partial}{\partial t}P(x,y;t) = L^{\mathrm{T}}P(x,y;t), \tag{6}$$

with

$$L^{\mathrm{T}} = \nabla_x[N_R\nabla_x - K_x] + \nabla_y[N_I\nabla_y - K_y]. \tag{7}$$

L^{T} is the formal adjoint (transpose) of L with respect to the bilinear (not hermitian) pairing

$$\langle P, f\rangle = \int f(x,y)P(x,y)\,dx\,dy, \tag{8}$$

i.e.,

$$\langle P, Lf\rangle = \big\langle L^{\mathrm{T}}P, f\big\rangle. \tag{9}$$

To understand the relation between the real and the complex measures one has to consider the evolution of a complex density $\rho(x)$ on $\mathcal{M}$ under the following complex FPE:

$$\frac{\partial}{\partial t}\rho(x;t) = L_0^{\mathrm{T}}\rho(x;t), \tag{10}$$

where now the complex Fokker–Planck operator L_0^{T} is

$$L_0^{\mathrm{T}} = \nabla_x\big[\nabla_x + \big(\nabla_x S(x)\big)\big]. \tag{11}$$

We will also use a slight generalization: for any $y_0 \in \mathcal{M}$ we consider the complex Fokker–Planck operator $L_{y_0}^{\mathrm{T}}$ given by

$$L_{y_0}^{\mathrm{T}} = \nabla_x\big[\nabla_x + \big(\nabla_x S(x+iy_0)\big)\big]. \tag{12}$$

$L_{y_0}^{\mathrm{T}}$ is the formal adjoint of

$$L_{y_0} = \big[\nabla_x - \big(\nabla_x S(x+iy_0)\big)\big]\nabla_x. \tag{13}$$

The complex density

$$\rho(x;\infty) \propto \exp\big[-S(x)\big] \tag{14}$$

is a stationary solution of (10), which is expected to be unique. Numerical studies (where feasible) of (10) confirm this; in fact the convergence to the limit (14) seems to be exponentially fast.

We have to make a few technical remarks about the space of observables we choose: all observables have to be entire holomorphic functions; we will furthermore require that their restrictions to the real submanifold $\mathcal{M}_r$ span a large enough space $\mathcal{D}$.

(1) If $\mathcal{M}_r = T^n$, $\mathcal{D}$ should be a dense subset of $\mathcal{C}(\mathcal{M}_r)$, the set of all continuous functions on $\mathcal{M}$ equipped with the norm $\|\mathcal{O}\| \equiv \sup_x |\mathcal{O}(x)|$; a good choice is the space of finite linear combinations of exponentials.
(2) If $\mathcal{M}_r = \mathbb{R}^n$ and the action S has a real part that grows at least like $|x|$ as $|x| \to \infty$, the functions in $\mathcal{O} \in \mathcal{D}$ should be bounded polynomially and dense in the Banach space defined by the norm $\|\mathcal{O}\| \equiv \sup_x \exp(-|x|)|\mathcal{O}(x)|$; a natural choice for $\mathcal{D}$ is the space of polynomials.
(3) If $\mathcal{M}_r = \mathbb{R}^n$ and the action is purely imaginary, one has to find a submanifold $\mathcal{M}_r' \subset \mathcal{M}_c$ which is a suitable deformation of $\mathcal{M}_r$ into the complex domain, such that the integral of $\exp(-S)$ converges and $\mathcal{M}_r'$ can still be parameterized by $x \in \mathbb{R}^n$. The conditions on the observables, expressed in this parameterization are then as in (2). In a slight abuse of language, we still refer to $\mathcal{M}_r'$ as the 'real submanifold'. Again polynomials are a natural choice for the space of observables.

We set

$$\langle\mathcal{O}\rangle_{P(t)} \equiv \frac{\int O(x+iy)P(x,y;t)\,dx\,dy}{\int P(x,y;t)\,dx\,dy} \tag{15}$$

and

$$\langle\mathcal{O}\rangle_{\rho(t)} \equiv \frac{\int O(x)\rho(x;t)\,dx}{\int \rho(x;t)\,dx}. \tag{16}$$

What one would like to show is that

$$\langle\mathcal{O}\rangle_{P(t)} = \langle\mathcal{O}\rangle_{\rho(t)}, \tag{17}$$

if the initial conditions agree,

$$\langle\mathcal{O}\rangle_{P(0)} = \langle\mathcal{O}\rangle_{\rho(0)}, \tag{18}$$

which is ensured provided

$$P(x,y;0) = \rho(x;0)\delta(y-y_0). \tag{19}$$

One expects that in the limit $t \to \infty$ the dependence on the initial condition disappears by ergodicity.

To establish a connection between the 'expectation values' with respect to ρ and P for a suitable class of observables, one moves the time evolution from the densities to the observables and makes use of the Cauchy–Riemann (CR) equations. Formally, i.e. without worrying about boundary terms and existence questions, this works as follows: first we use the fact that we want to apply the complex operators L_{y_0} only to functions that have analytic continuations to all

of $\mathcal{M}_c$. On those analytic continuations we may act with the Langevin operator

$$\tilde{L} \equiv \big[\nabla_z - \big(\nabla_z S(z)\big)\big]\nabla_z, \tag{20}$$

whose action on holomorphic functions agrees with that of L, since on such functions $\nabla_y = i\nabla_x$ and $\Delta_x = -\Delta_y$ so that the difference $L - \tilde{L}$ vanishes.

We now use $\tilde{L}$ to evolve the observables according to the equation

$$\partial_t \mathcal{O}(z;t) = \tilde{L}\mathcal{O}(z;t) \quad (t \geq 0), \tag{21}$$

with the initial condition $\mathcal{O}(z;0) = \mathcal{O}(z)$, which is formally solved by

$$\mathcal{O}(z;t) = \exp[t\tilde{L}]\mathcal{O}(z). \tag{22}$$

In (21, 22), because of the CR equations, the tilde may be dropped, and we will do so now. So we also have

$$\mathcal{O}(z;t) = \exp[tL]\mathcal{O}(z). \tag{23}$$

In [21] it was shown that $\mathcal{O}(z;t)$ is holomorphic if $\mathcal{O}(z;0)$ is. The evolution can therefore also be obtained equivalently by solving

$$\partial_t \mathcal{O}(x+iy_0;t) = L_{y_0}\mathcal{O}(x+iy_0;t) \quad (t \geq 0) \tag{24}$$

and subsequent analytic continuation.

The crucial object to consider is, for $0 \leq \tau \leq t$,

$$F(t,\tau) \equiv \int P(x,y;t-\tau)\mathcal{O}(x+iy;\tau)\,dx\,dy, \tag{25}$$

which interpolates between the ρ and the P expectations:

$$F(t,0) = \langle\mathcal{O}\rangle_{P(t)}, \qquad F(t,t) = \langle\mathcal{O}\rangle_{\rho(t)}. \tag{26}$$

The first equality is obvious, while the second one can be seen as follows, using (19, 23):

$$\begin{aligned} F(t,t) &= \int P(x,y;0)\big(e^{tL}\mathcal{O}\big)(x+iy;0)\,dx\,dy \\ &= \int \rho(x;0)\big(e^{tL_0}\mathcal{O}\big)(x;0)\,dx \\ &= \int \mathcal{O}(x;0)\big(e^{tL_0^{\mathrm{T}}}\rho\big)(x;0)\,dx \\ &= \langle\mathcal{O}\rangle_{\rho(t)}, \end{aligned} \tag{27}$$

where it is only necessary to assume that integration by parts in x does not produce any boundary terms.

The desired result (17) would follow if $F(t,\tau)$ were independent of τ. To check this, we take the τ derivative:

$$\begin{aligned} &\frac{\partial}{\partial\tau}F(t,\tau) \\ &\quad = -\int \big(L^{\mathrm{T}}P(x,y;t-\tau)\big)\mathcal{O}(x+iy;\tau)\,dx\,dy \\ &\qquad + \int P(x,y;t-\tau)L\mathcal{O}(x+iy;\tau)\,dx\,dy. \end{aligned} \tag{28}$$

Integration by parts, if applicable without boundary term at infinity, then shows that the two terms cancel, hence $\frac{\partial}{\partial\tau}F(t,\tau) = 0$ and thus proves (17), irrespective of N_I.

Notice that here we have found a place where the formal argument may fail: if the decay of the product

$$P(x,y;t-\tau)\mathcal{O}(x+iy;\tau) \tag{29}$$

and its derivatives is insufficient for integration by parts without boundary terms. We shall return to this in Sect. 4.

If (28) vanishes and furthermore

$$\lim_{t\to\infty}\langle\mathcal{O}\rangle_{\rho(t)} = \langle\mathcal{O}\rangle_{\rho(\infty)}, \tag{30}$$

with $\rho(\infty)$ given by (14), one can conclude that the expectation values of the Langevin process relax to the desired values. Equation (30) will be ensured when the spectrum of $L_{y_0}^{\mathrm{T}}$ lies in a half plane $\mathrm{Re}\,z \leq 0$ and 0 is a nondegenerate eigenvalue.[2] The numerical evidence in practically all cases points to the existence of a unique stationary probability density $P(x,y;\infty)$.[3] More detailed information about this will be given below.

In [21] three questions were raised. The first one concerned the exponentiation of the operators $L, \tilde{L}$ and their transposes, or in other words whether they are generators of semigroups on some suitable space of functions. Even though we have not found a general mathematical answer to this question, numerics indicate that it is affirmative in all cases considered; for L_{y_0} in our first toy model a proof will be given in the Appendix. Likewise it is not known whether the spectra of L, L_{y_0} are contained in the left half plane and if 0 is a nondegenerate eigenvalue, but the numerics again strongly indicate an affirmative answer.

So the main remaining question concerns the integrations by parts without boundary terms, which underlie the shifting of the time evolution from the measure to the observables and back; actually what is really needed is the ensuing τ independence of $F(t,\tau)$, defined in (25). A crucial role

[2] Actually, convergence of $P(x,y;t)$ is more than what is really needed, because the measure will only be tested against holomorphic observables.

[3] Note, however, that in [16] dependence on initial conditions was found. This is due to peculiar features of the classical flow pattern, leading to degenerate equilibrium distributions. On the other hand, observables are independent of initial conditions (and agree with the exactly known results).

for the correctness of CLE simulations is therefore played by the vanishing of (28). Whether this holds or not will be studied in detail for one of our toy models in Sect. 4.1.

3 A criterion for correctness

As explained in the previous section, $F(t,\tau)$ has to be independent of τ for all times t, i.e.,

$$\frac{\partial}{\partial\tau}F(t,\tau)=0. \tag{31}$$

Below in Sect. 4.1 it will be seen that for the U(1) one-link model the τ derivative is largest at $\tau=0$. This motivates to try the superficially weaker condition

$$\lim_{t\to\infty}\frac{d}{d\tau}F(t,\tau)\bigg|_{\tau=0}=0. \tag{32}$$

Equation (32) is clearly weaker than (31), but as we will see later, it is still sufficient for correctness, modulo some technical conditions, if it holds for a sufficiently large set of observables.

If we now look again at (28), we realize that for the equilibrium measure (always assuming it exists) $L^{\mathrm{T}}P(x,y;\infty)=0$ and hence the first term on the right hand side vanishes. The criterion (32) thus turns into

$$E_{\mathcal{O}}\equiv\int P(x,y;\infty)\tilde{L}\mathcal{O}(x+iy;0)\,dx\,dy=\langle\tilde{L}\mathcal{O}\rangle=0, \tag{33}$$

where we used the fact that on $\mathcal{O}$ L and $\tilde{L}$ can be used interchangeably. This would of course also follow from the equilibrium condition $L^{\mathrm{T}}P(x,y;\infty)=0$ on $\mathcal{M}_c$, if the decay of P at large y is sufficient to allow integration by parts on $\mathcal{M}_c$ without boundary term. Equation (33) is a fairly simple condition that is rather easy to check for a given observable and constitutes one of the main results of this paper. Note, however, that it has to be satisfied for 'all' observables, i.e. for a basis (in a suitable sense) of our chosen space $\mathcal{D}$, so it represents really an infinite tower of identities.

It may be worth noting that the collection of identities (33), applied to all observables, is closely related to the Schwinger–Dyson equations (SDE). We show this for the simple case of a scalar theory on a lattice with fields denoted by ϕ_i: the SDEs are well known to arise from the relation

$$\left\langle\frac{\partial f}{\partial\phi_i}\right\rangle=\left\langle f\frac{\partial S}{\partial\phi_i}\right\rangle \tag{34}$$

for 'any' function f of the fields (in most applications the observables are chosen to be exponentials $\exp(\sum_i\phi_i j_i)$). Our Langevin criterion $\langle\tilde{L}\mathcal{O}\rangle=0$ on the other hand reads

$$\sum_i\left\langle\frac{\partial^2\mathcal{O}}{\partial\phi_i^2}\right\rangle=\sum_i\left\langle\frac{\partial\mathcal{O}}{\partial\phi_i}\frac{\partial S}{\partial\phi_i}\right\rangle. \tag{35}$$

It is quite obvious that (34) implies (35): take $f=\partial_i\mathcal{O}$ in (34). The converse is also easy: one has to find a set of observables $\mathcal{O}_j$ satisfying

$$\sum_i\frac{\partial^2\mathcal{O}_j}{\partial\phi_i^2}=\partial_j f; \tag{36}$$

this involves the inversion of the (functional) Laplace operator, which is always possible here, because the only zero modes are constants.

We proceed to show that in principle the identities for a sufficiently large (countably infinite) set of observables are also sufficient to ensure correctness, provided a certain bound is satisfied. Let us now assume that we have, by whatever method, obtained a measure Q on $\mathcal{M}_c$ that allows integration of all $\mathcal{O}\in\mathcal{D}$ and furthermore satisfies a bound

$$\big|\langle Q,\mathcal{O}\rangle\big|\le C\|\mathcal{O}\|, \tag{37}$$

where C is some constant and the norm is the one discussed in Sect. 2 (recall that this norm only involved the values of $\mathcal{O}$ on $\mathcal{M}_r$). We claim that modulo certain technical conditions the fulfillment of (33) for a basis of $\mathcal{D}$,

$$\langle Q,\tilde{L}\mathcal{O}\rangle=\int Q(x,y)\tilde{L}\mathcal{O}(x+iy)\,dx\,dy=0, \tag{38}$$

implies that the Q expectations are correct, i.e.

$$\begin{aligned}\langle Q,\mathcal{O}\rangle&=\int Q(x,y)\mathcal{O}(x+iy)\,dx\,dy\\&=\frac{1}{Z}\int_{\mathcal{M}_r}\mathcal{O}(x)e^{-S(x)}\,dx.\end{aligned} \tag{39}$$

The argument uses the fact that the values of $\mathcal{O}$ on $\mathcal{M}_r$ already determine the values on $\mathcal{M}_c$. So $\langle Q,\mathcal{O}\rangle$ can be viewed as a linear functional on the space $\mathcal{D}$ considered as functions on $\mathcal{M}_r$, which is assumed to be dense in $\mathcal{C}(\mathcal{M}_r)$. Because of the bound (37) this functional has a unique extension to a linear functional on all of $\mathcal{C}(\mathcal{M}_r)$. By a standard theorem of analysis—the Riesz–Markov theorem (see for instance [23])—this linear functional is therefore given by a complex measure $\sigma_Q dx$ on $\mathcal{M}_r$, i.e. we can write

$$\langle Q,\mathcal{O}\rangle=\int_{\mathcal{M}_r}\mathcal{O}(x)\sigma_Q(x)\,dx, \tag{40}$$

where σ_Q is allowed to contain δ functions. Since $\mathcal{O}$ was any observable, it may be replaced by $\tilde{L}\mathcal{O}$; this yields

$$\langle Q,\tilde{L}\mathcal{O}\rangle=\int_{\mathcal{M}_r}(L\mathcal{O})(x)\sigma_Q(x)\,dx=0, \tag{41}$$

which is equivalent to

$$\int_{\mathcal{M}_r}\mathcal{O}(x)\big(L_0^{\mathrm{T}}\sigma_Q\big)(x)\,dx=0, \tag{42}$$

using only integration by parts on $\mathcal{M}_r$, which in general unproblematic, because either $\mathcal{M}_r$ is compact or there is strong decay on $\mathcal{M}_r$. Since this holds for all $\mathcal{O}$ in the dense set $\mathcal{D}$, we conclude

$$L_0^{\mathrm{T}}\sigma_Q = 0. \tag{43}$$

To deduce from this that $\sigma_Q = \exp(-S)/Z$, 0 has to be a nondegenerate eigenvalue of L_0^{T}, an assumption which had to be made in Sect. 2 in any case. If, on the other hand, $E_{\mathcal{O}} \neq 0$ for some observable $\mathcal{O}$, the simulation cannot be correct. Since by formal integration by parts on $\mathcal{M}_c$ the equilibrium condition $L^{\mathrm{T}}P(x, y; \infty) = 0$ would imply $E_{\mathcal{O}} = 0$, we can see only one possible reason for $E_{\mathcal{O}} \neq 0$, namely insufficient falloff of the equilibrium measure in imaginary direction.

There are of course some fine points of functional analysis, but they need not concern us here, since checking the bound (37) will in general be too hard anyway, except in some toy models (see the Appendix). Here the goal is to arrive at some criteria that are easy to use in practice.

It is well known that the SDE's have spurious unphysical solutions, see for instance [9, 24, 25]. This should be obvious from the fact that they are equivalent to a (functional) differential equation which requires at least some kind of boundary condition for definiteness and also from the fact that they are *recursive* relations that can always be fulfilled by fixing the low moments/modes in an arbitrary way. So it has to be checked whether requiring the criterion (33) in fact selects the correct expectation values. The bound (37) will in general be sufficient for this. In the Appendix we will see how this works in the U(1) one-link model.

4 Testing etiology and diagnostics in toy models

4.1 Numerical study of $F(t, \tau)$ in the U(1) one-link model

The U(1) one-link model was introduced in [11] and studied further in [21]. At lowest order in the hopping expansion it is defined by the action

$$S = -\beta \cos z - \kappa \cos(z - i\mu) = -a\cos(z - ic), \tag{44}$$

with

$$a = \sqrt{(\beta + \kappa e^{\mu})(\beta + \kappa e^{-\mu})}, \tag{45}$$

$$c = \frac{1}{2}\ln\frac{\beta + \kappa e^{\mu}}{\beta + \kappa e^{-\mu}}, \tag{46}$$

leading to the drift

$$K_x = -\mathrm{Re}\, S' = -a\sin x \cosh(y - c), \tag{47}$$

$$K_y = -\mathrm{Im}\, S' = -a\cos x \sinh(y - c). \tag{48}$$

It is easy to see by shifting an integration contour that no essential generality is lost if we set $c = 0$, which we will do in the sequel.[4] We also set $a = 1$.

A natural choice of a basis for the space of observables are the exponentials e^{ikz}. Here we study in detail the question whether the quantity $F(t, \tau)$, see (25), is indeed independent of τ, as required for correctness. We use both the CLE and the FPE for this analysis. In order to be able to solve the FPE, we use complex noise ($N_I > 0$)[5] and impose a cutoff in the y-direction.[6] This cutoff is introduced in the simplest possible way, namely by imposing periodic boundary conditions in field space. We denote the value of the cutoff by Y, such that $-Y \leq y \leq Y$. Periodizing the observable of course violates the Cauchy–Riemann (CR) equations at the 'seam', while the drift becomes discontinuous across the 'seam'. Therefore such a cutoff destroys the formal argument for correctness. However, using the nonuniqueness of the positive measure on $\mathcal{M}_c$ there is still a chance to get correct results with such a measure; we will check whether this is possible by tuning the cutoff. Indeed, here it is important to realize that if (31) holds, the equality (17) follows and thus the correctness of the CLE method is ensured. The results presented below suggests that such a naive cutoff procedure can be justified to some extent by its success, at least in this model.

We present the results of a numerical evolution of the function $F(t, \tau)$, choosing the simplest observable $\mathcal{O} = \exp(iz)$ and the parameter $N_I = 0.1$. To do this, both the evolution of the probability density $P(x, y; t)$, see (6), and the evolution of the observable, see (21, 24), are needed.

- $P(x, y; t - \tau)$ is obtained by using the time dependent FPE in the Fourier representation; a simple Euler discretization in time with time step 10^{-5} turns out to be sufficient [21].
- $\mathcal{O}(x + iy; \tau)$ is obtained as described in the previous section, see (21, 24), by using the evolution of $\mathcal{O}$ under $\tilde{L}$ or equivalently under L_{y_0}. This evolution does not depend on either N_I or the cutoff Y, since neither L nor L_{y_0} depend on those two parameters.
- $F(t, \tau)$ is then obtained by summing up the products of $\mathcal{O}(x + iy; t)$ and $P(x, y; t - \tau)$.

The results are presented in Figs. 1, 2, 3, 4. In these plots we show $F(t, \tau)$ as a function of τ, for a number of t values,

[4] When $c = 0$, the action is real and there is no sign problem. Therefore we use complex noise to keep the dynamics complexified. With real noise, there are no issues in this model (as opposed to the case of the XY model [15]).

[5] Note that $N_I = 0$, which should be preferred for a CLE simulation, cannot be used for the FPE computations, because it would lead to instabilities. However, already a very small N_I appears to be sufficient to stabilize the FPE.

[6] The x direction is periodic.

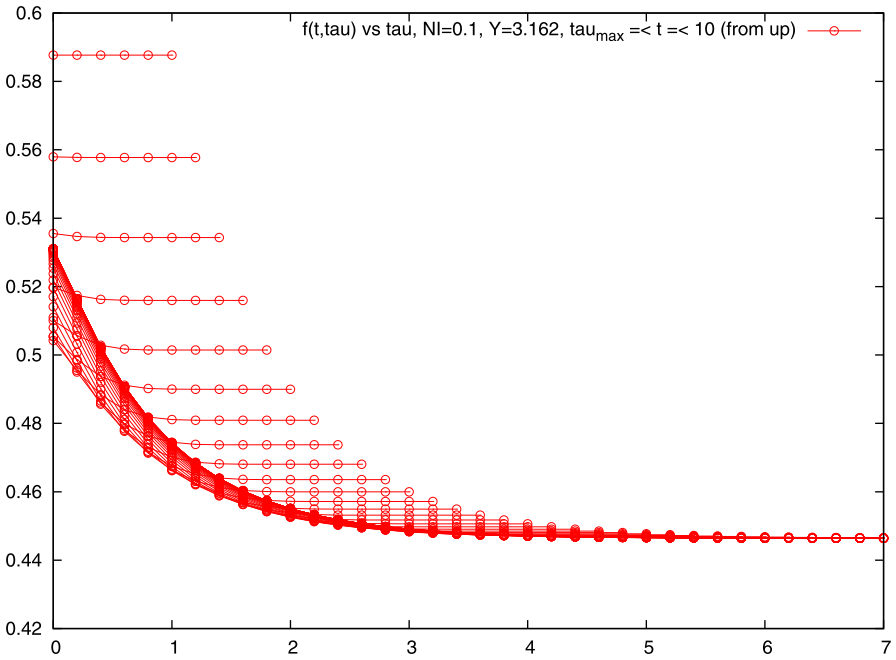

Fig. 1 U(1) one-link model: $F(t,\tau)$ vs. τ for several values of t, with $0 < \tau < t$, $N_I = 0.1$ and the cutoff $Y = 3.162$

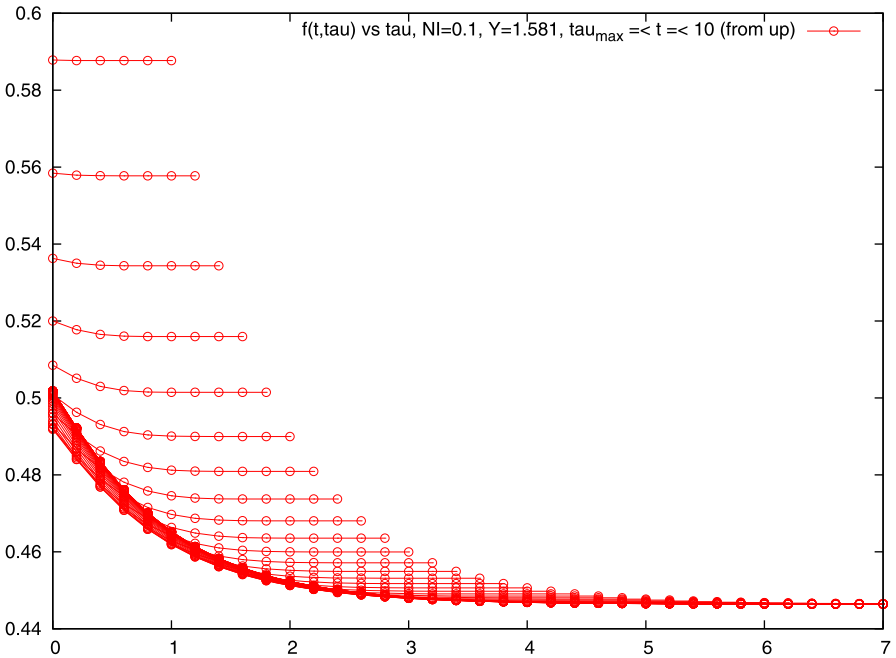

Fig. 2 As in Fig. 1, with $Y = 1.582$

ranging from $t = 1$ to $t = 7$. For every t value, τ runs from 0 to t. In all cases $N_I = 0.1$, while the cutoff Y varies from $Y = 3.162$ in Fig. 1 to $Y = 0.158$ in Fig. 4.

The following features can be seen from the figures:

1. In general $F(t,\tau)$ is *not* independent of τ.
2. The dependence is always strongest at $\tau = 0$.
3. The sign of the τ derivative changes somewhere between $Y = 0.474$ and $Y = 1.582$; there seems to be a 'best choice' of cutoff at which the derivative vanishes.

This picture is corroborated by Fig. 5, which shows directly the τ derivatives obtained as finite difference approximations. In this figure we also show different values of N_I and it is clearly visible that for very small values of N_I the derivative also effectively vanishes. To sum up: we find numerically that the formal argument for correctness generally fails for $N_I \neq 0$ because of the first feature above. In Appendix we analyze the mathematical reasons for this failure.

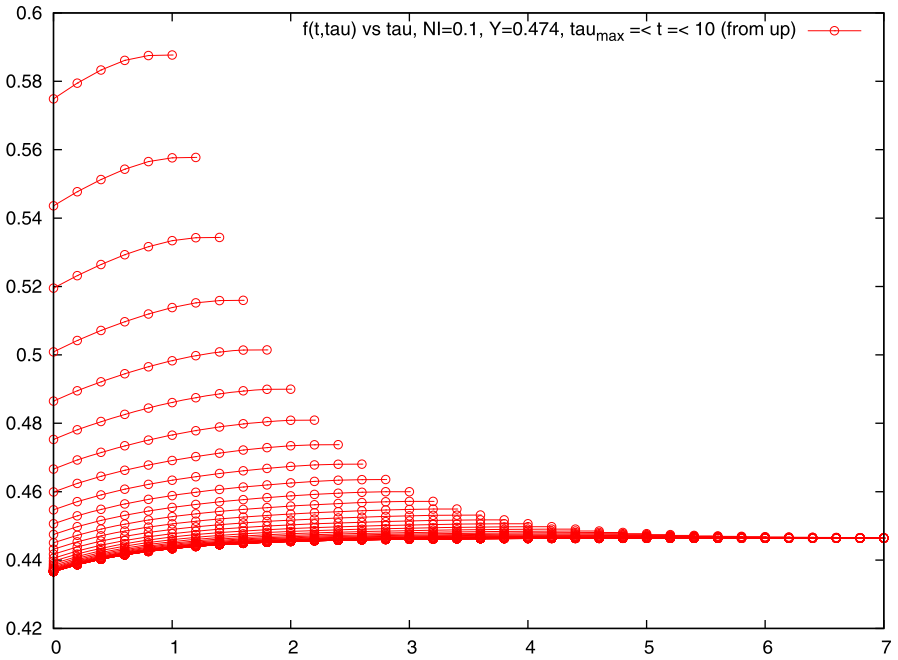

Fig. 3 As in Fig. 1, with $Y = 0.474$

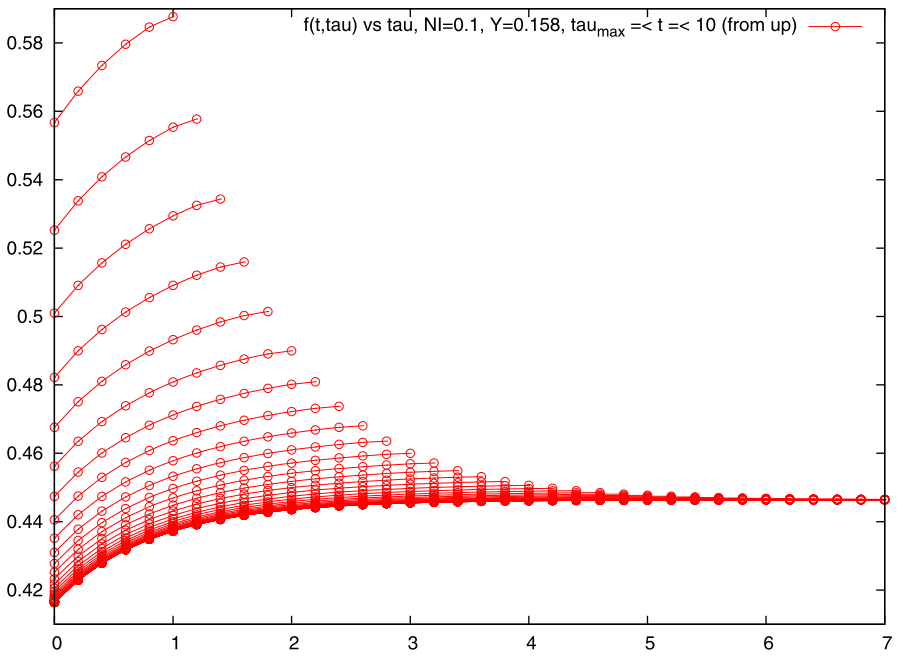

Fig. 4 As in Fig. 1, with $Y = 0.158$

4.2 Falloff of the equilibrium measures

In this subsection we study the $t \to \infty$ limit of $P(x, y; t)$, i.e. the equilibrium measure, in order to check why and how our general criterion (33) can fail. As remarked in Sect. 3, the equilibrium condition

$$L^{\mathrm{T}} P(x, y; \infty) = 0 \tag{49}$$

implies fulfillment of the criterion

$$E_{\mathcal{O}} \equiv \int P(x, y; \infty) \tilde{L}\mathcal{O}(x + iy; 0)\, dx\, dy = 0, \tag{50}$$

provided integration by parts on $\mathcal{M}_c$ without boundary terms at imaginary infinity is justified. So the falloff of $P(x, y; \infty)$ is crucial for success or failure.

U(1) one-link model For the U(1) one-link model we are able to make rather precise statements about the falloff of the equilibrium measure in the y direction. The system is symmetric under the reflections $x \mapsto -x$ and $y - c \mapsto -(y - c)$.

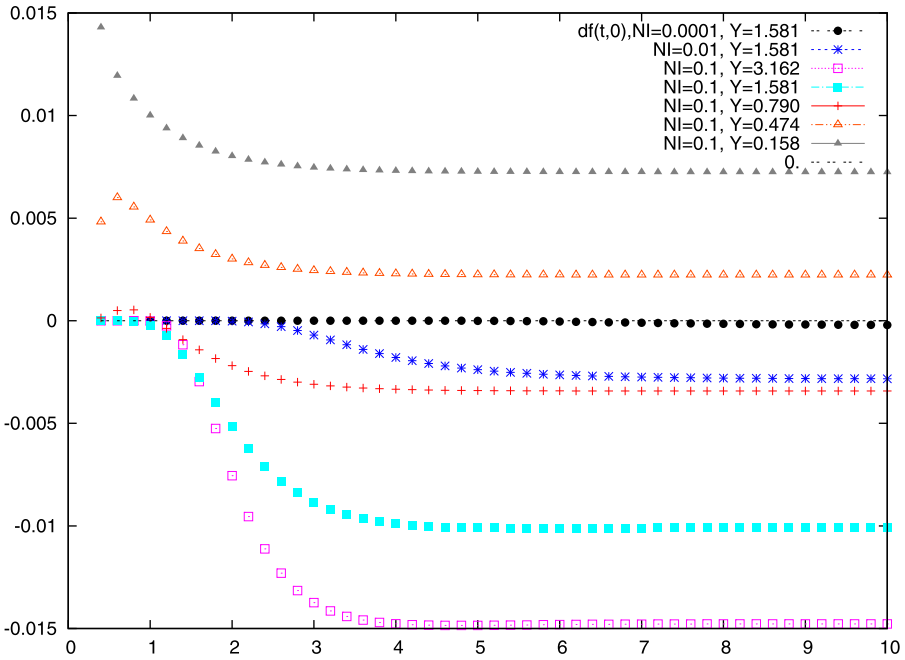

Fig. 5 U(1) one-link model: τ derivative of $F(t,\tau)$ as a function of τ at $t = 10$ for several values of the cutoff Y and complex noise parameter N_I

To study the falloff of the equilibrium measure in y we again chose $c = 0$ and grouped the data obtained by the CLE simulation into bins $|y| \in [(n - 1/2)\Delta, (n + 1/2)\Delta)$ with $\Delta = 0.1$. For clarity we chose rather large values of N_I, namely $N_I = 0.1, 0.5, 1.0$ and 9.0. The results are shown in Fig. 6 and show a universal decay rate

$$P(x, y; \infty) \sim \exp\bigl(-2|y|\bigr). \tag{51}$$

This result improves considerably the statement made in [21] and explains the difficulties with determining reliably expectation values of $\exp(ikz)$ for $|k| \geq 2$ (they are suffering from extremely large fluctuations).

We also consider the Fourier modes [21]

$$\widehat{P}_k(y; t) = \int dx\, e^{ikx} P(x, y; t), \tag{52}$$

which are closely related to the expectation values of the exponentials via

$$\bigl\langle e^{ikz} \bigr\rangle = \int dy\, \widehat{P}_k(y; t) e^{-ky}, \tag{53}$$

using the fact that

$$\int dy\, \widehat{P}_0(y; t) = \int dx\, dy\, P(x, y; t) = 1. \tag{54}$$

We simplify the notation for $\widehat{P}_k(y; \infty)$ to $\widehat{P}_k(y)$. By binning in y as above we also produced estimates of the modes $\widehat{P}_k(y)$ for $k = 1, 2$ and $N_I = 1$, shown in Fig. 7. $\widehat{P}_2$ seems already to be quite noisy, but at least the first few kinks visible in the figure for $\widehat{P}_2$ correspond to true sign changes. But what is more important is the clearly visible fact that $\widehat{P}_1$ and $\widehat{P}_2$ decay at least like $\exp(-3|y|)$. This can be confirmed using the stationary Fokker–Planck equation (FPE) obeyed by $P(x, y; \infty)$. In terms of the Fourier modes the FPE reads

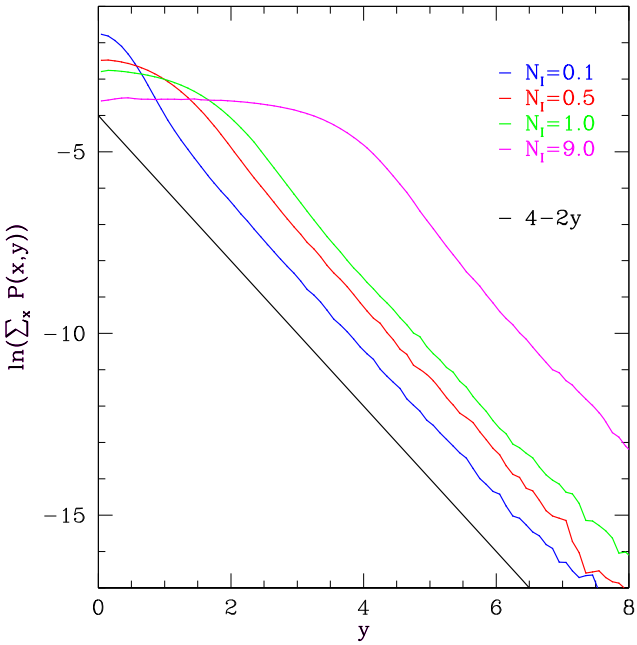

Fig. 6 Logarithmic histograms of the equilibrium measures for the U(1) one-link model

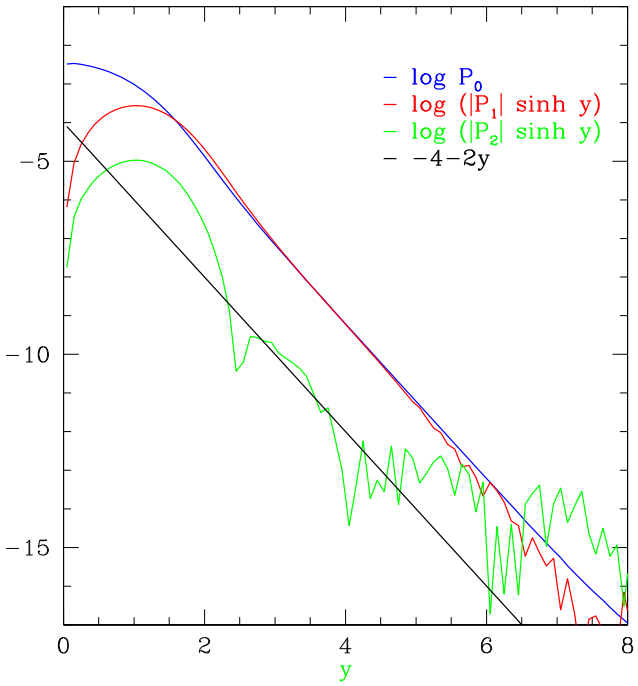

Fig. 7 Logarithmic histograms of the low modes of the equilibrium measures for the U(1) one-link model

(see (65) of [21])

$$\begin{aligned}&\big(N_R k^2 - N_I \partial_y^2\big)\widehat{P}_k(y)\\&\quad+\frac{\beta}{2}\cosh(y)\big[(k-1)\widehat{P}_{k-1}(y)-(k+1)\widehat{P}_{k+1}(y)\big]\\&\quad-\frac{\beta}{2}\sinh(y)\partial_y\big[\widehat{P}_{k-1}(y)+\widehat{P}_{k+1}(y)\big]=0.\end{aligned}\tag{55}$$

Since we are interested in the large $|y|$ asymptotics, we may replace $\cosh(y)$ and $\sinh(y)$ by $\pm 1/2\exp(|y|)$. Integrating (55) for $k=0$ from 0 to y and using evenness in y we obtain

$$N_I\widehat{P}_0'(y)+\frac{\beta}{2}e^{|y|}\widehat{P}_1(y)=0.\tag{56}$$

So if $\widehat{P}_0$ decays like $\exp(-2|y|)$, $\widehat{P}_1$ will decay like $\exp(-3|y|)$. Continuing inductively and assuming exponential decay, one obtains easily

$$\widehat{P}_k(y)\sim c_k e^{-(|k|+2)|y|}.\tag{57}$$

Unfortunately (55) also implies that $c_{k+1}\sim kc_k$, which means that one cannot sum up the asymptotic behavior of the $\widehat{P}_k$ to obtain the asymptotics of $P(x,y;\infty)$.

More important is what we learn about the expectation values of $\exp(ikz)$, which should be given by

$$\big\langle e^{ikz}\big\rangle=\int P(x,y;\infty)e^{ikx-ky}\,dx\,dy.\tag{58}$$

The integral on the right hand side does not converge absolutely for $|k|\geq 2$, hence its value is ambiguous. A well defined result may be obtained by first integrating over x, but it is not clear if this corresponds to the long-time average of the complex Langevin process. But it seems that the large fluctuations observed in the CLE data reflect the fact that the integral is ill defined. One can also try to compute expectation values using the binning employed above. This corresponds to first integrating over x, then over y. The results agree with those obtained directly by the CLE simulation (up to some loss of precision due to the finite width of the bins), which is of course no surprise, as the binning is based on the CLE simulation.

The conclusion is that the CLE process with complex noise and without a field cutoff will in general not produce unambiguous results for the expectation values of exponentials $\exp(ikz)$ with higher $|k|$.

Guralnik–Pehlevan model To see if this phenomenon of slow decay of the equilibrium distribution is not just a specialty of our U(1) one-link model, we also analyzed the equilibrium measure for the simplest polynomial model (called GP model in the sequel), studied by Guralnik and Pehlevan [22] and discussed briefly before [21].

The model is defined by the action

$$S=-i\beta\left(z+\frac{1}{3}z^3\right);\tag{59}$$

since this action is purely imaginary, we have to deform the real axis to a path (submanifold) $\mathcal{M}_r$ as described in Sect. 2 such that $\exp(-S)$ is absolutely integrable over $\mathcal{M}_r$. A possible choice [22] is the path $z=x+i\epsilon\sqrt{1+x^2}$ for some small positive ϵ.

Since the action produces a stable fixed point at $x=0$, $y=1$, we produced histograms representing $P(x,y;\infty)$ by binning $r=\sqrt{x^2+(y-1)^2}$ in intervals of length 0.1. They are shown in Fig. 8. Since in this case we expect a power falloff, we use a log–log scale. The indications are again that the rate of falloff is the same for different values of $N_I>0$, namely roughly like $r^{-1.5}$, whereas for $N_I=0$ we find a stronger falloff (we cannot decide at this point whether it is still power-like or stronger). Accepting this observation one concludes that for $N_I>0$ again the higher moments $\langle z^k\rangle$ of the equilibrium distribution are ill defined, a fact that is reflected by large fluctuations of these quantities in the CLE simulations [21].

4.3 Testing the criterion

We now proceed to test the truncated version of our criterion on the two toy models introduced; our primary interest is to see whether checking it only for a few low moments (modes) is sufficient to identify incorrect results.

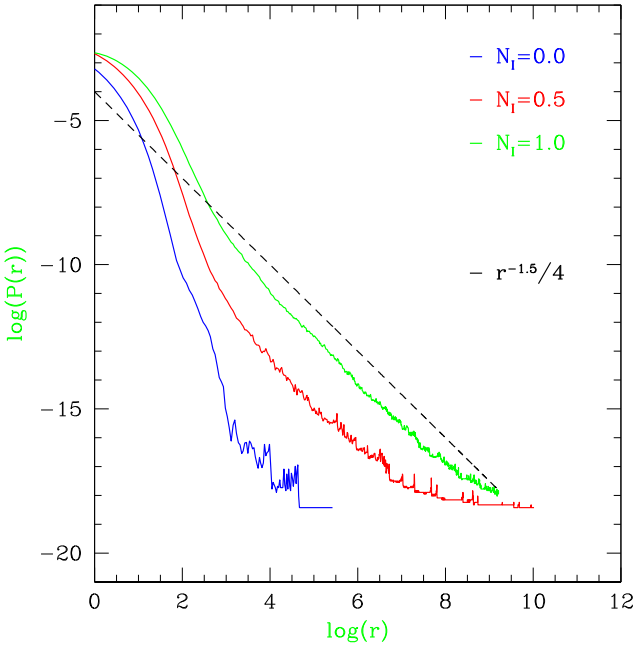

Fig. 8 Histograms of the equilibrium measures for the GP model on a log–log scale

U(1) one-link model For this model we consider the two cases

$$\beta = 1, \qquad \kappa = 0, \tag{60}$$

and

$$\beta = 1, \qquad \kappa = 0.25, \qquad \mu = 0.5 \tag{61}$$

(which is equivalent to $\beta \approx 1.27, \kappa = 0$). In both cases we chose $N_I = 0.1$ which leads to manifestly incorrect results for the CLE simulation without cutoff. We introduce a periodic cutoff Y in imaginary direction, which makes it possible to use the FPE and also stabilizes the CLE expectation values [21].

Using the FPE as well as the CLE simulations, we measure the expectation values

$$c_k \equiv \langle \mathcal{O}_k \rangle = \big\langle \exp(ikz) \big\rangle, \tag{62}$$

as well as the indicators

$$E_k \equiv \big\langle \tilde{L} \exp(ikz) \big\rangle, \tag{63}$$

both for $k = 1, 2, 3$. In Figs. 9 and 10 we show $\langle \mathcal{O}_k \rangle$ divided by its exact value minus 1 as well as E_k, for $k = 1, 2, 3$. The results indicate the remarkable fact that at a particular value of the cutoff not only all the indicators E_k vanish but also the observables c_k agree with their exact values (it should be noted that due to the symmetry of the system the observables $\exp(-iz)$ and $\exp(-2iz)$ do not contain any extra information). Note that E_2 has a second zero, but at that point $E_1 \neq 0$.

So in this case our simple test of the identity (33) for two observables is apparently sufficient to identify an incorrect simulation: it has sufficient sensitivity to reject wrong solutions. To make sure that at the properly tuned cutoff value the measure P is indeed correct, one would in principle have to check all exponentials, which is a practical impossibility.

In our U(1) one-link model the SDE hierarchy amounts just to the well-known recursion relation for the Bessel functions $I_k(\beta)$ and it is determined by fixing $\langle 1 \rangle = 1$ and $\langle \exp(iz) \rangle = c_1$. In a CLE simulation c_1 will depend on the value of the cutoff. If

$$c_1 \neq \frac{I_1(\beta)}{I_0(\beta)}, \tag{64}$$

the SDE recursion rapidly runs away to infinity and it is manifest that the bound (37) cannot hold. So this bound seems to be crucial for picking out the right solution of the SDE. On the other hand the cutoff models in general obey the bound, but unless the cutoff is tuned correctly, they will miss the right value of c_1 and fail to obey the SDE recursion.

Guralnik-Pehlevan model We next apply our test to the GP model. Since this model has noncompact real and imaginary parts, we introduce *two* periodic cutoffs: X for the real and Y for the imaginary part.

In this model $\tilde{L} = \partial_z^2 + i\beta(1 + z^2)\partial_z$, and the first few relations read

$$\begin{aligned} E_1 &\equiv \langle \tilde{L} z \rangle = i\beta \big\langle 1 + z^2 \big\rangle, \\ E_2 &\equiv \big\langle \tilde{L} z^2 \big\rangle = 2\big\langle 1 + i\beta z \big(1 + z^2\big) \big\rangle, \\ E_3 &\equiv \big\langle \tilde{L} z^3 \big\rangle = 3\big\langle 2z + i\beta z^2 \big(1 + z^2\big) \big\rangle, \end{aligned} \tag{65}$$

leading to SD relations between the expectation values of z^k.

It is easy to see that the exact results [22], which can be expressed in terms of Airy functions, indeed satisfy these relations. For example, for $\beta = 1$ one finds $\langle z \rangle \approx 1.1763i$, $\langle z^2 \rangle = -1$, $\langle z^3 \rangle \approx -0.1763i$.

We measured the moments $c_k \equiv \langle z^k \rangle$ for $k = 1, 2, 3, 4$; this allows us also to obtain $E_2 = \langle \tilde{L} z^2 \rangle$ and $E_3 = \langle \tilde{L} z^3 \rangle$; note that $E_1 = \langle \tilde{L} z \rangle = i + i\langle z^2 \rangle = 0$ is already tested by comparing $\langle z^2 \rangle$ to its exact values -1. In Fig. 11 we present the results obtained for $N_I = 1$ and a fixed cutoff $X = 3.17$ in the x direction, both by using the FPE and the CLE simulation. For this value of N_I it was observed [21] that the CLE without cutoff does *not* reproduce the correct values. The figure, on the other hand, shows that there is a value of the y cutoff (near $Y = 0.8$) for which the two criteria $E_2 = E_3 = 0$ are fulfilled and also the right values for the moments c_1, c_2, c_3, c_4 are obtained.

With purely real noise ($N_I = 0$) the situation is quite different. For this case the FPE simulation is unstable: Fig. 12

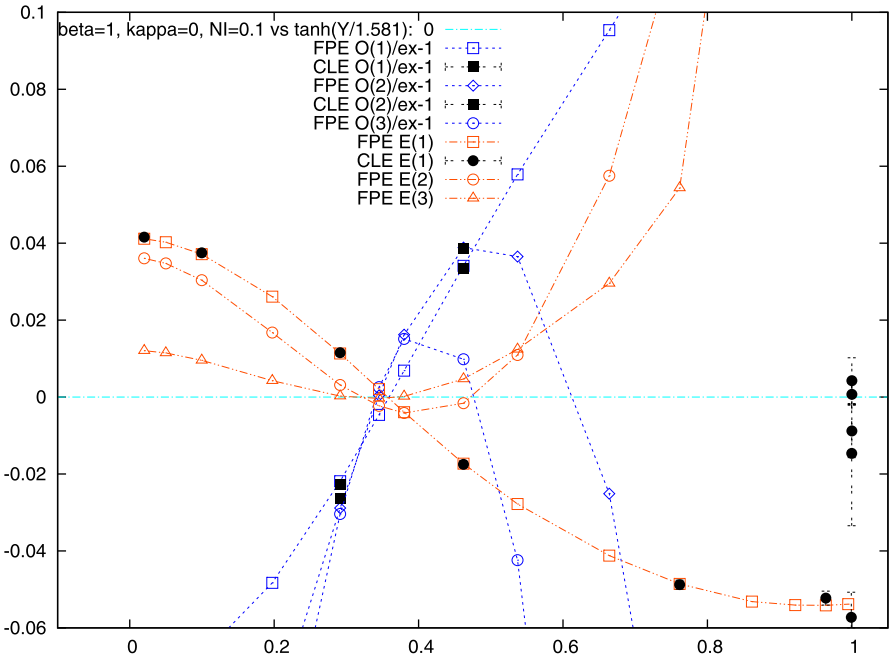

Fig. 9 Cutoff (Y) dependence of various quantities in the U(1) one-link model, for $\beta = 1$, $\kappa = 0$, $N_I = 0.1$. See main text for further details

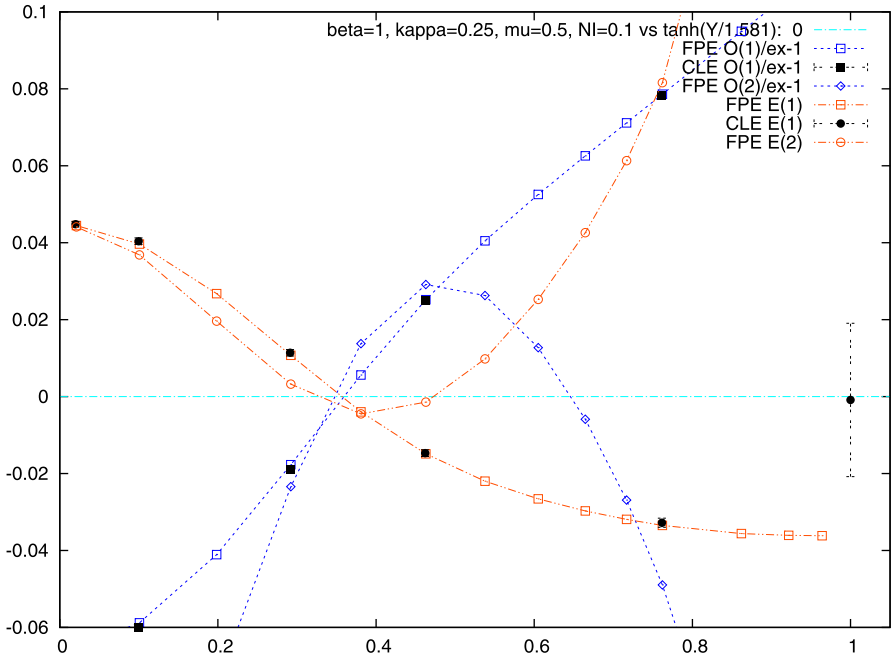

Fig. 10 As in Fig. 9, for $\beta = 1$, $\kappa = 0.25$ and $\mu = 0.5$

shows the time evolution of the FPE for $N_I = 0$; the evolution settles onto metastable values very close to the exact ones, but then takes off and diverges. For comparison we also show the FPE time evolutions for two rather small nonzero values: $N_I = 0.01$ and $N_I = 0.1$ (all three figures are using the cutoffs $X = Y \approx 3.95$). As seen in Figs. 12, 13, a small amount of imaginary noise is sufficient to stabilize the evolution, at least for the times considered. This seems to conform at least qualitatively to the discussion found in Numerical Recipes Ch. 19 [27]. Quantitatively from that discussion one would expect that much larger values of N_I are needed for stabilization; however, this does not seem to be the case here (actually for such large values of N_I the FPE simulation becomes unstable again). Already with this small nonzero N_I one obtains good convergence to the exact result, provided the cutoff is not extremely small.

The CLE simulation, on the other hand, works perfectly for $N_I = 0$. We have seen already in Sect. 3 that for $N_I = 0$ the equilibrium distribution is quite well concentrated and shows a very strong falloff. In agreement with this, we find

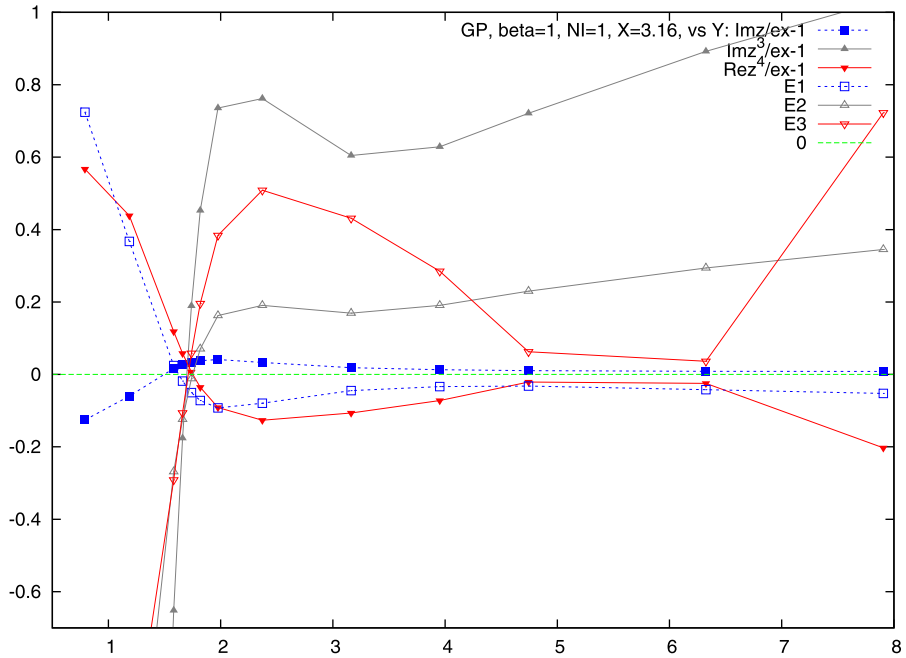

Fig. 11 GP model: cutoff dependence for $\beta = 1$, $N_I = 1$

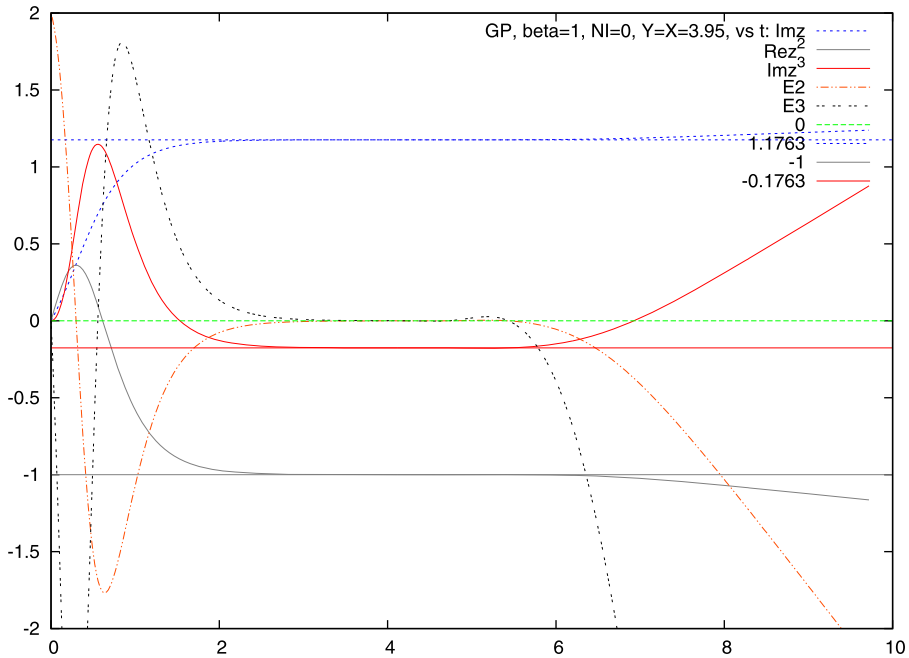

Fig. 12 FPE evolution in the GP model: t dependence of various quantities for $N_I = 0$, $\beta = 1$ and cutoffs $X = Y = 3.95$. See main text for more details

that the data are quite insensitive to the cutoffs introduced; for $X = 3.95$ as before, even a cutoff of $Y = 0.8$ is sufficient to produce values close to the exact ones and consequently also fulfill the criteria $E_1 = E_2 = E_3 = 0$ with good precision. These facts can be clearly seen in Fig. 14; in this figure we display for comparison the CLE results for $N_I = 0$ and the FPE results for $N_I = 0.01$.

We conclude that our simple test seems to have sufficient sensitivity to select the right simulation.

5 Conclusions

In this paper we have identified the reasons why the CLE simulations sometimes fail to produce correct expectation values, namely insufficient falloff of the probability distribution and too strong growth of the observables in the imaginary directions. These two features invalidate the formal steps required to show equivalence between the CLE results and the ones defined with respect to the original complex measure.

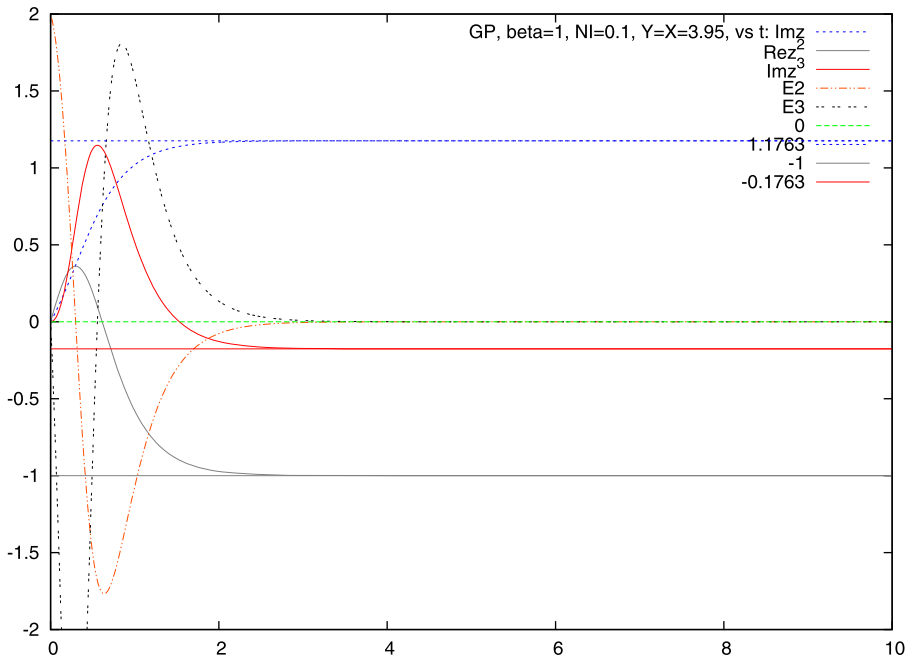

Fig. 13 As in Fig. 13 for $N_I = 0.1$

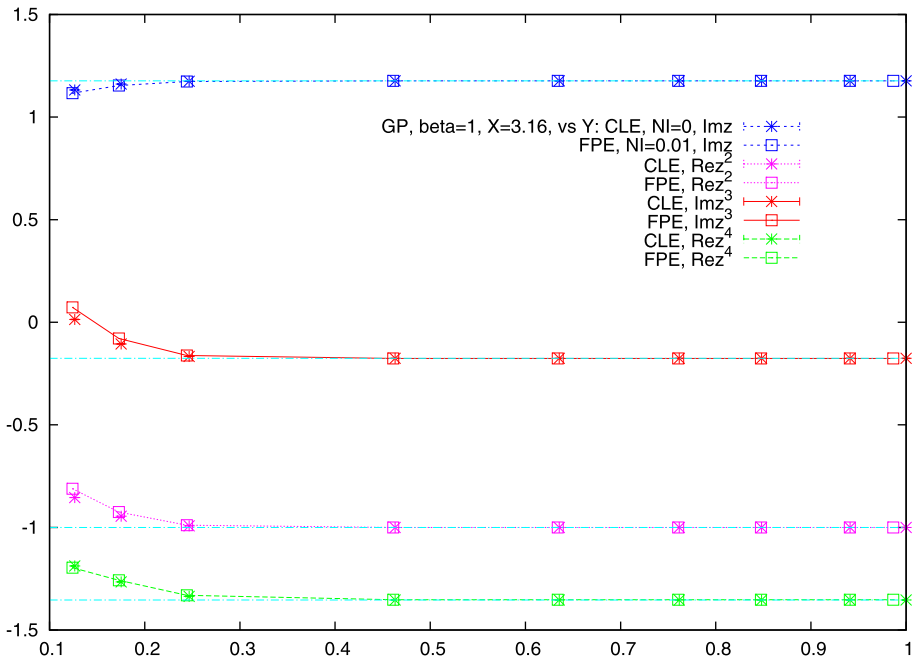

Fig. 14 GP model: cutoff (Y) dependence for $\beta = 1$ and $N_I = 0$ (CLE) and $N_I = 0.01$ (FPE)

We formulated a simple set of criteria, one for each observable $\mathcal{O}$, of the form $\langle \tilde{L}\mathcal{O} \rangle = 0$, where $\tilde{L}$ is a Langevin operator expressed in terms of the drift terms appearing in the CLE. A violation of these criteria implies that the results obtained from the CLE are incorrect. This test is of obvious use in realistic cases where the exact results are not known and also holds in field theory. Besides indicators of a wrong result, we found that the criteria also demonstrate a very strong sensitivity, i.e. when they are fulfilled, the results are correct (as far as it can be checked). This is true in all cases considered here as well as in the XY model, where a comparison with a worldline formulation is available [15].

In the two toy models studied in this paper two parameters affect the outcome of a simulation, namely the amount of complex noise ($N_I > 0$) and the presence of a variable cutoff in field space. In general, complex noise and the presence of a cutoff will lead to incorrect results and a violation of the criteria. However, by tuning both, we found that we are able to satisfy the criteria and reproduce the exact results, demonstrating the sensitivity of the truncated test cri-

terion, in addition to the specificity which holds on general grounds.

A continuation of a study of the issues discussed in this paper and an application to lattice models is currently in progress.

Acknowledgements I.-O. S. thanks the MPI for Physics München and Swansea University for hospitality. G. A. and F. A. J. are supported by STFC.

Appendix: Mathematical analysis in the U(1) one-link model

In the Appendix we analyze in more detail the behavior of the time-evolved observables in order to understand why $F(t,\tau)$ is not independent of τ in general, using for illustration the help of the U(1) one-link model.

We describe the evolution of the observables in some more detail: the Langevin operator $\tilde{L}$ is

$$\tilde{L} = \frac{d^2}{dz^2} - a\sin(z-ic)\frac{d}{dz}. \tag{66}$$

For the observables e^{ikz} we find

$$\tilde{L}e^{ikz} = -k^2 e^{ikz} - \frac{a}{2}k\big(e^{c}e^{i(k+1)z} - e^{-c}e^{i(k-1)z}\big). \tag{67}$$

Choosing now $c=0$ and $a=\beta$, we consider an observable

$$\mathcal{O}(z) = \sum_k a_k e^{ikz} \tag{68}$$

and its time evolution $\mathcal{O}(z;t) \equiv \sum_k a_k(t)e^{ikz}$ defined by (21). This evolution can be expressed in terms of the coefficients a_k as

$$\partial_t a_k(t) = -k^2 a_k(t) + \frac{\beta}{2}\big[-(k-1)a_{k-1}(t) + (k+1)a_{k+1}(t)\big], \tag{69}$$

and may be viewed as evolution under $\tilde{L}$, L or, if we fix $y=0$, as evolution under L_0. The evolution operator L_0 in Fourier space is thus represented by a tridiagonal matrix with elements

$$(\widehat{L}_0)_{kk'} = -k^2\delta_{kk'} + \frac{\beta}{2}\big[-(k-1)\delta_{k-1,k'} + (k+1)\delta_{k+1,k'}\big]. \tag{70}$$

We now establish the following facts:

1. The Langevin operators L_{y_0} generate exponentially bounded semigroups on the Hilbert space $L^2(dx)$ for any y_0. In particular there are no poles.
2. If the Fourier transform of $\mathcal{O}$ contains only positive modes, this will also be true for $\exp(tL_{y_0})\mathcal{O}$. But typically then all positive modes will be populated.
3. $$\lim_{t\to\infty} e^{tL_{y_0}}\mathcal{O} = \frac{1}{Z_{y_0}}\int dx\, \mathcal{O}(x+iy_0)e^{-S(x+iy_0)}. \tag{71}$$
   The convergence is exponentially fast.
4. For holomorphic observables $\mathcal{O}$
   $$\exp(tL)\mathcal{O} = \exp(tL_{y_0})\mathcal{O}. \tag{72}$$
   Since the right hand side is independent of $N_I = N_R - 1$, so is the left hand side. This argument does not involve any integration by parts.
5. $\mathcal{O}(x+iy;t)$ grows for $t>0$ more strongly than any exponential as $y\to\infty$, invalidating integration by parts except for $N_I = 0$.

The proof of (1) follows from a theorem to be found in [26] (Theorem 11.4.5). The point is that the drift (first order in derivatives) term of L_{y_0} is a so-called Phillips perturbation of the Laplacian:

$$L_{y_0} = A + B, \tag{73}$$

with

$$A = \frac{d^2}{dx^2}, \qquad B = \beta\sin(x+iy_0)\frac{d}{dx}. \tag{74}$$

B can be applied to any vector of the form $\exp(tA)\psi$, $t>0$ and we have

$$\int_0^1 dt\, \big\|B\exp(tA)\big\| < \infty. \tag{75}$$

These two properties allow to set up a perturbation expansion for $\exp[t(A+B)]$ and show its convergence. Explicitly

$$e^{t(A+B)} = e^{tA} + \sum_{n=1}^{\infty}\int_{0\le t_1\le\cdots\le t_n\le t} e^{t_1 A} \times Be^{(t_2-t_1)A}B\cdots Be^{(t-t_n)A}. \tag{76}$$

Convergence in norm is not hard to see: by Fourier transformation one sees that

$$\left\|\frac{d}{dx}e^{tA}\right\| = \sup_k\big|ke^{-tk^2}\big| \le \frac{1}{\sqrt{2te}}, \tag{77}$$

hence

$$\big\|Be^{tA}\big\| \le \mathrm{const}\beta e^{|y_0|}\frac{1}{\sqrt{t}}. \tag{78}$$

From this is it obvious that the bound (75) holds; since the integration volume in (75) is $t^n/n!$, the series converges in norm.

Item (2) is obvious.

Item (3) means in particular that the evolution of $\mathcal{O}$ converges to a constant. While it is obvious that all constants are eigenfunctions of L_{y_0}, we do not have sufficient analytic understanding of the spectra of the operators L_{y_0} to prove this convergence. Numerically, however, it is seen easily that the evolution converges to the correct constant and the convergence is exponentially fast.

Item (4) is an obvious consequence of analyticity.

Item (5) is seen by numerically analyzing the growth of the coefficients $a_k(t)$ for $t > 0$: Using the initial condition $a_1 = 1$, $a_k = 0$ for $k \neq 0$ and $\beta = 1$ as before, $a_k(t)$ are the Fourier coefficients of $\exp(tL_0)\mathcal{O}_1$ with $\mathcal{O}_1(x) = \exp(ix)$. In Fig. 15 we plot $-\ln(|a_k(t)|)/k$ for four different times ($t = 0.5, 1, 2, 3$) against $\ln(k)$. As remarked, only positive modes get populated; it turns out that the coefficients $a_k(t)$ alternate in sign. From this we conclude that $|\mathcal{O}_1(z;t)|$ grows most for large negative y and is maximal for $x = \pm\pi$. Modes were cut off at $|k| = 50$, but the picture shows for all the times clearly an asymptotic linear increase with a slope close to 1, so we conclude

$$a_k(t) \sim K^k(-1)^k k^{-\gamma k}, \tag{79}$$

with γ possibly slightly less than 1 and some constant K. Further numerical studies show that the behavior of (79) is universal: it is independent of the initial condition and β. For comparison in this figure we also show (in black) the quantity $\ln(k!)/k + \ln(2)$, which seems to be approached asymptotically by the other curves.

Since (79) obviously implies

$$\big|a_k(t)\big| \geq K^k k^{-k}, \tag{80}$$

by a simple argument we can conclude that $\mathcal{O}(x + iy; t)$ grows superexponentially in y direction: we put $w = e^z$; then, using only positive modes for the initial conditions, $\mathcal{O}(z;t)$ is given by the power series

$$\mathcal{O}(z;t) = \sum_{k=0}^{\infty} a_k(t) w(z)^k. \tag{81}$$

Cauchy's estimate says that for any $R \geq 0$

$$\big|a_k(t)\big| \leq S(R) R^{-k}, \tag{82}$$

where

$$S(R) = \sup_{|w|=R} \big|\mathcal{O}\big(z(w);t\big)\big| = \sup_x \big|\mathcal{O}(x - i\ln R; t)\big|. \tag{83}$$

From this and our numerics we conclude that asymptotically

$$S(R) \geq (KR)^k k^{-k} \tag{84}$$

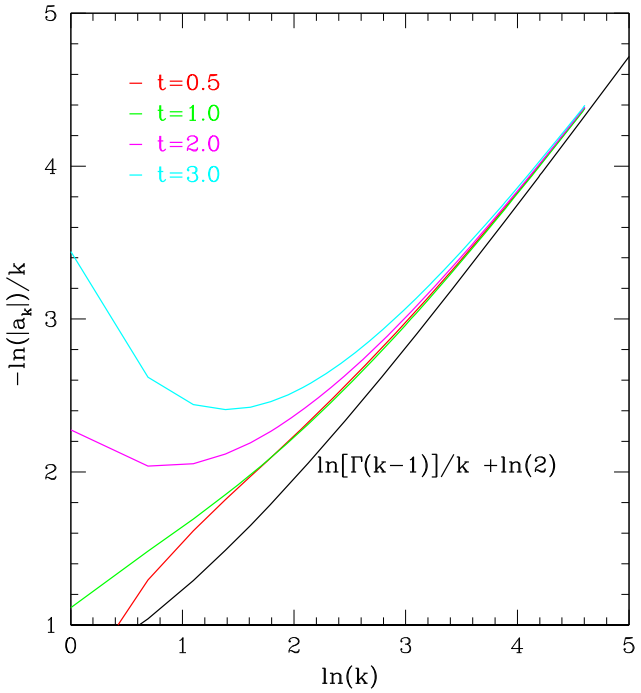

Fig. 15 U(1) one-link model: asymptotics of the Fourier coefficients $a_k(t)$

and this holds for any k. The optimal value is

$$k_0 = (KR)e^{-1}, \tag{85}$$

which leads to the bound

$$S\big(e^{-y}\big) = \big|\mathcal{O}(\pi + iy)\big| \geq \exp\big[\text{const}\exp(-y)\big]. \tag{86}$$

Note that this holds in particular for $y < 0$! Since for $N_I > 0$ and $t, \tau > 0$ one can at best expect a Gaussian decay of $P(x, y; t)$, (25) in this case involves an integral of a function that is not absolutely integrable and hence its value is ambiguous, depending on the order of integrations. Thus the formal argument for correctness of the CLE fails.

References

1. P. de Forcrand, Proc. Sci. **LAT2009**, 010 (2009). 1005.0539 [hep-lat]
2. J. Klauder, Acta Phys. Austriaca Suppl. **XXXV**, 251 (1983)
3. J. Klauder, J. Phys. A, Math. Gen. **16**, L317–L319 (1983)
4. J. Klauder, Phys. Rev. A **29**, 2036–2047 (1984)
5. G. Parisi, Phys. Lett. B **131**, 393 (1983)
6. F. Karsch, H.W. Wyld, Phys. Rev. Lett. **55**, 2242 (1985)
7. P.H. Damgaard, H. Hüffel, Phys. Rep. **152**, 227 (1987)
8. J. Berges, I.-O. Stamatescu, Phys. Rev. Lett. **95**, 202003 (2005). hep-lat/0508030
9. J. Berges, S. Borsanyi, D. Sexty, I.O. Stamatescu, Phys. Rev. D **75**, 045007 (2007). hep-lat/0609058
10. J. Berges, D. Sexty, Nucl. Phys. B **799**, 306 (2008). 0708.0779 [hep-lat]

11. G. Aarts, I.-O. Stamatescu, J. High Energy Phys. **0809**, 018 (2008). 0807.1597 [hep-lat]
12. G. Aarts, Phys. Rev. Lett. **102**, 131601 (2009). 0810.2089 [hep-lat]
13. G. Aarts, J. High Energy Phys. **0905**, 052 (2009). 0902.4686 [hep-lat]
14. G. Aarts, F.A. James, E. Seiler, I.O. Stamatescu, Phys. Lett. B **687**, 154 (2010). 0912.0617 [hep-lat]
15. G. Aarts, F.A. James, J. High Energy Phys. **1008**, 020 (2010). 1005.3468 [hep-lat]
16. G. Aarts, K. Splittorff, J. High Energy Phys. **1008**, 017 (2010). 1006.0332 [hep-lat]
17. J. Ambjorn, S.K. Yang, Phys. Lett. B **165**, 140 (1985)
18. J.R. Klauder, W.P. Petersen, J. Stat. Phys. **39**, 53 (1985)
19. H.Q. Lin, J.E. Hirsch, Phys. Rev. B **34**, 1964 (1986)
20. J. Ambjorn, M. Flensburg, C. Peterson, Nucl. Phys. B **275**, 375 (1986)
21. G. Aarts, E. Seiler, I.O. Stamatescu, Phys. Rev. D **81**, 054508 (2010). 0912.3360 [hep-lat]
22. G. Guralnik, C. Pehlevan, Nucl. Phys. B **822**, 349 (2009). 0902.1503 [hep-lat]
23. M. Reed, B. Simon, *Functional Analysis*, vol. I. (Academic Press, New York, 1972)
24. E. Seiler, *Untersuchung eines selbstgekoppelten relativistischen Skalarfeldes mit Funktionalmethoden*. Doctoral thesis, Technische Universität München (1971, unpublished) (in German)
25. C. Pehlevan, G. Guralnik, Nucl. Phys. B **811**, 519 (2009). 0710.3756 [hep-th]
26. E.B. Davies, *Linear Operators and their Spectra* (Cambridge University Press, Cambridge, 2007)
27. W.H. Press et al., *Numerical Recipes in Fortran 77—The Art of Scientific Computing*, 2nd edn. (Cambridge University Press, Cambridge, 1992). Ch. 19